



Cite this: *Chem. Commun.*, 2019, 55, 4427

Received 17th January 2019,
Accepted 22nd March 2019

DOI: 10.1039/c9cc00437h

rsc.li/chemcomm

An imidazole-functionalised cage is synthesised that can coordinate to Cu(i). X-ray analysis reveals a T-shaped coordination of copper by the imidazole ligands reminiscent of the coordination geometry found in enzymatic active sites. This cage complex can catalyse the oxidation of benzylic alcohols to benzaldehydes utilizing oxygen as the terminal oxidant.

The coordination of imidazole moieties from histidines to copper ions plays a key role in many enzymatic active sites. Examples are particulate methane monooxygenases (pMMO),^{1,2} lytic polysaccharide monooxygenases (LPMO)¹ and tyrosinases (Ty, Fig. 1a-c).³ These offer fascinating reactivities and selectivities that can often not be achieved by man-made catalysts. Chemists are inspired to develop (functional) molecular compounds that mimic these active sites. This mimicking has mostly been devoted towards the first coordination sphere, resulting in coordination complexes of rather low molecular weight.⁴⁻⁷

In comparison, the design of cavity-based metal complexes has received way less attention.^{8,9} This approach may allow to mimic also features of the active site pocket. It may also grant the advantages of chemistry in synthetic cages, such as protection of the catalytic active centre, stabilization of highly reactive species, control of binding events and unusual selectivities.¹⁰

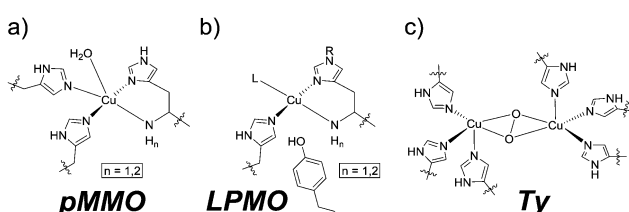


Fig. 1 Active sites of (a) pMMO, (b) LPMO and (c) Ty.

Institut für Anorganische Chemie, Universität Göttingen, Tammannstraße 4, 37077 Göttingen, Germany. E-mail: matthias.otte@chemie.uni-goettingen.de
 † Electronic supplementary information (ESI) available: Experimental details. CCDC 1868264 and 1876236. For ESI and crystallographic data in CIF or other electronic format see DOI: 10.1039/c9cc00437h

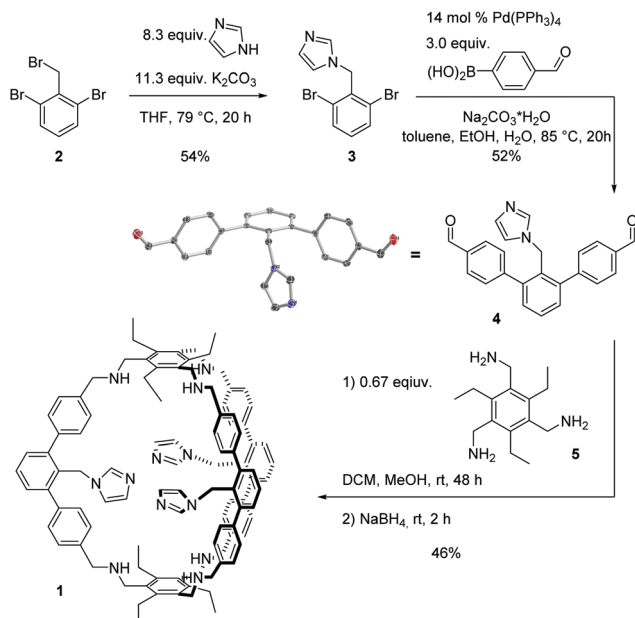
To date, the mimicking of enzymatic active sites containing histidine by imidazole-functionalised cavity based ligands is mainly dominated by cyclodextrins and calix[6]arenes where the metal is actually located outside of the cavity with its binding site pointing towards it.¹¹ Notably, it has been demonstrated very recently that imidazole-functionalised metal organic frameworks are able to coordinate to copper resulting in active catalysts for the conversion of methane to methanol.¹²

While active sites of enzymes containing metalloporphyrins have been mimicked by the use of molecular cage compounds,¹³ examples of molecular cages that offer such a well-defined ligand sphere to mimic non-heme enzymatic active sites *via* imidazole coordination are yet unprecedented. This is surprising as *endo*-functionalised organic cages have been shown to bind catalytic active centers.¹⁴ Costas and Ribas and co-worker recently synthesised Zn-, Cu- and Fe-coordination complexes based on pyridine coordination within a self-assembled nanocage.¹⁵ However, these species have not been reported to be catalytically active for the transformation of organic substrates.

Here we present the synthesis and characterization of the aza-cyclophane **1** (Scheme 1) and show that it is able to coordinate to copper(i) resulting in a catalyst for the oxidation of benzylic alcohols. Cage **1** was synthesised from known **2** (Scheme 1). *Via* nucleophilic substitution with an imidazolium salt, **3** was obtained in a yield of 54%. Afterwards, a Suzuki-Miyaura-coupling gave the imidazole-functionalised building block **4** in 52% yield. Single crystals suitable for X-ray diffraction analysis were obtained by layer diffusion of pentane into a dichloromethane solution of **4**. **4** and the known compound **5** were subject to a reductive amination protocol with the aim to obtain **1**. Such an approach is well documented for the synthesis of organic cages.¹⁶ After stirring a CH₂Cl₂/CH₃OH solution of **4** and **5** for 2 days at room temperature and subsequent addition of sodium borohydride and purification, cage **1** was isolated in 46% yield.

1 was characterised *via* ESI-MS, ¹H, ¹H DOSY, ¹³C NMR and IR spectroscopy. The ESI-MS reveals signals with *m/z* values of 1501.8892, 751.4488 and 501.3016 corresponding to **1** + H⁺,

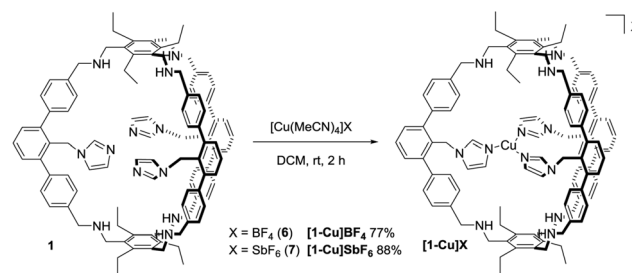




Scheme 1 Synthesis of cage **1** and molecular structure of **4** in the solid state.

1 + 2H⁺ and **1** + 3H⁺. In the ¹H NMR spectrum, two singlets are found at chemical shifts of 3.90 and 3.88 ppm that indicate the presence of benzylic amines (Fig. 2a). Three signals with relative integrals of three hydrogens each corresponding to the hydrogens of the imidazoles are observed, showing the imidazole's equivalence on NMR-timescale. The ¹H DOSY NMR spectrum (see ESI†) reveals only one molecule size apart from solvents and trace amounts of grease. A diffusion coefficient of 4.1×10^{-10} m² s⁻¹ is found in chloroform. Using the Stokes-Einstein equation for spherically shaped molecules, this diffusion coefficient translates to a hydrodynamic radius of 9.8 Å.

With **1** in hand, we studied its behaviour to act as ligand for copper(i) (Scheme 2). Reaction with 0.9 equivalents Cu(MeCN)₄BF₄ (**6**) in dichloromethane at room temperature allows for the isolation of **[1-Cu]BF₄** as a white solid in 77% yield. The ¹H NMR spectrum of



Scheme 2 Synthesis of **[1-Cu]BF₄** and **[1-Cu]SbF₆**.

[1-Cu]BF₄ shows remarkable changes compared to the one of **1** (Fig. 2b). All three signals that are assigned to the imidazole protons (labelled with A–C) shift upon addition of **6**. These shifts indicate that a coordination of the imidazole to copper was successful and that all imidazoles behave identically on NMR-timescale. Solutions of **[1-Cu]BF₄** turn greenish within minutes upon stirring under air (see ESI† for UV Vis spectra). The NMR spectrum of **[1-Cu]BF₄** changes significantly. No separated signals corresponding to the imidazole protons and the methylene-bridge could be assigned caused by broadening of all signals (see ESI†). A less pronounced broadening is observed for the backbone signals further indicating a coordination of copper to the imidazole moieties. The ¹H DOSY NMR spectrum (see ESI†) of **[1-Cu]BF₄** in chloroform shows a single compound with a diffusion coefficient of 4.1×10^{-10} m² s⁻¹ which translates to a hydrodynamic radius of 9.9 Å. These values are close to the ones obtained from the ¹H DOSY NMR spectrum of **1**, which indicates that copper-coordination does not lead to any dimeric or oligomeric species. ESI-MS investigations of **[1-Cu]BF₄** shows species with *m/z* values of 1563.8112, 782.4088 and 1652.8288 corresponding to **[1-Cu]⁺**, **[1-Cu]⁺ + H⁺** and **[1-Cu]BF₄ + H⁺**.

X-ray analysis of single crystals of **[1-Cu]BF₄**, obtained by slow diffusion of THF into a diethylether solution, lead to a low data quality (see ESI†). However, the overall connectivity of the cage and its coordination to copper by all three imidazole units in the solid state could be confirmed. To obtain data of higher quality, we synthesised **[1-Cu]SbF₆** from **1** and Cu(MeCN)₄SbF₆ (**7**). NMR and MS gave analogous data compared to **[1-Cu]BF₄** (see ESI†). To our delight, we were able to obtain crystallographic data of higher quality by analysing single crystals of **[1-Cu]SbF₆** that form in a saturated ethereal solution at room temperature. As anticipated, copper is coordinated by each of the imidazole moieties (Fig. 3). A T-shaped coordination mode is found with N–Cu–N angles of 150°, 106° and 102°. Cu–N bond lengths of 1.9 Å are found for the imidazole units that are *trans* to each other, while the one for the remaining imidazole ligand is 2.1 Å. These values correspond well with the ones found in enzymatic active sites also showing a T-shaped coordination of the Cu(i) center. The Cu(i)–N(His) bond lengths in LPMOs are 1.9 Å, while the Cu(i)–NH₂ bond length is 2.1 Å.¹ The Cu(i)–N(His) bond lengths in the pMMO active site are 1.8 Å, 1.9 Å and 2.2 Å.¹⁷ The average distance between copper and the terminal carbon of the ethyl groups is 10 Å, which is in good

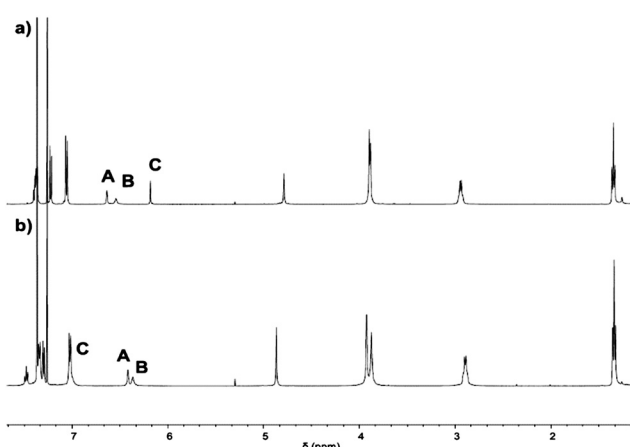


Fig. 2 ¹H NMR spectra of (a) **1** and (b) **[1-Cu]BF₄** in CDCl₃.



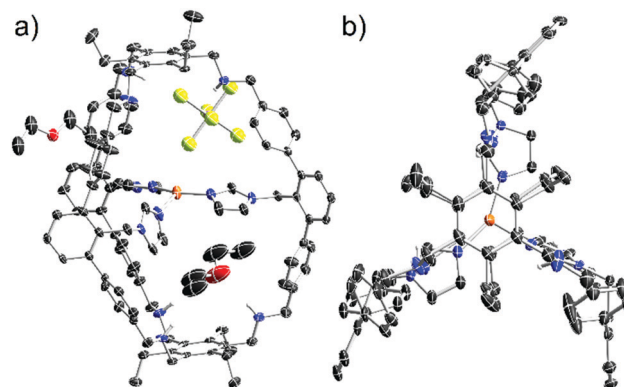


Fig. 3 Molecular structure of $[1\text{-Cu}]SbF_6$ in the solid state: (a) side view; (b) top view (solvent molecules and anion undisplaced). Carbon bonded hydrogen atoms are omitted for clarity.

agreement with the hydrodynamic radius obtained for $[1\text{-Cu}]BF_4$. For the SbF_6^- -counterion three different locations are found (see ESI†) with the two most populated being located on the cage face with the largest N–Cu–N bond angle. The obtained crystallographic data shows four possible positions for two diethylether molecules (see ESI†). Three of these are inside the cage cavity. Hydrogen bonding interactions are observed between the cage N–H moieties and the ether and the SbF_6^- anion as acceptors.

We next studied the ability of $[1\text{-Cu}]BF_4$ to catalyse the oxidation of organic substrates. We chose the oxidation of 4-methoxybenzyl alcohol (**8**) to 4-anisaldehyde (**9**) with catalytic amounts of TEMPO (2,2,6,6-tetramethylpiperidin-1-yl)oxyl in a DCM/water mixture under aerobic conditions as model reaction (Table 1).¹⁸ Performing the reaction for 1.5 h resulted in 7 turnovers (entry 1), while overnight reaction time led to 11 turnovers (entry 2). Increasing $[1\text{-Cu}]BF_4$ loading to 10 mol% resulted in 88% yield (entry 3), while increasing the substrate concentration to 0.50 M resulted in 28% yield (entry 4). Performing the reaction in absence of $[1\text{-Cu}]BF_4$ gave only

Table 1 $[1\text{-Cu}]BF_4$ -catalysed oxidation of **8** to **9**^a

Entry	Catalyst ([mol%])	Yield [%]	<i>t</i> [h]	Catalyst, cat. TEMPO	
				8	9
1	$[1\text{-Cu}]BF_4$ (1)	7	1.5		
2	$[1\text{-Cu}]BF_4$ (1)	11	14		
3	$[1\text{-Cu}]BF_4$ (10)	88	16		
4 ^b	$[1\text{-Cu}]BF_4$ (1)	28	14		
5	None	<1	14		
6	6 (1)	1	14		
7	1 (1)	0	14		
8 ^c	$[1\text{-Cu}]BF_4$ (1)	<1	14		
9 ^b	6.3(NMI) (1)	37	14		
10 ^b	10-(bipy)-2(NMI) (1)	39	14		

^a Substrate concentration = 0.11 M; all reactions under air; 7 mol% TEMPO; 11.1 equiv. H_2O rt; all yields were determined by 1H NMR spectroscopy of the crude product mixtures in presence of internal standards.

^b Substrate concentration = 0.50 M. ^c Without TEMPO. NMI = *N*-methylimidazole. bipy = 2,2'-bipyridine.

Table 2 Investigation of $[1\text{-Cu}]BF_4$ in competition experiments^a

Entry	[Cu] ([mol%])	R1	R2	PR1 : PR2		Yield [%]
				Me	<i>t</i> -Bu	
1	$[1\text{-Cu}]BF_4$ (1)	Me	<i>t</i> -Bu	59 : 41	6	
2	6.3(NMI) (1)			42 : 58	22	
3	10-(bipy)-2(NMI) (0.6)			52 : 48	21	
4	$[1\text{-Cu}]BF_4$ (1)	H	<i>t</i> -Bu	67 : 33	7	
5	6.3(NMI) (1)			55 : 45	4	
6	10-(bipy)-2(NMI) (0.6)			52 : 48	3	

^a Substrate concentration = 0.11 M; reactions under air; 7 mol% TEMPO; 11.1 equiv. H_2O ; rt; 5.0 h. All yields were determined by 1H NMR spectroscopy of the crude product mixtures in presence of internal standards. NMI = *N*-methylimidazole. bipy = 2,2'-bipyridine.

traces of **9** (entry 5). Control experiments with copper salt **6**, empty cage **1** or without TEMPO showed no or only very little formation of **9** (maximum yield = 1%; entries 6 to 8). These results show that $[1\text{-Cu}]BF_4$ is capable of oxidising organic substrates at room temperature in a catalytic fashion *via* employing oxygen as terminal oxidant. For the transformation of **8** to **9** the catalytic performance of $[1\text{-Cu}]BF_4$ is comparable to other copper based systems. Using **6** in the presence of three equivalents of *N*-methylimidazole (NMI) gave **9** in 37% yield (entry 9),¹⁹ while $Cu(MeCN)_4OTf$ (**10**) with 2,2'-bipyridine (bipy) and *N*-methylimidazole gave 39% yield (entry 10).¹⁸

We were wondering if $[1\text{-Cu}]BF_4$ may have the ability to discriminate between substrates in competition experiments, especially compared to **6.3(NMI)** and **10-(bipy)-2(NMI)**. When a 1 : 1 mixture of 3,5-di-methylbenzyl alcohol and 3,5-di-*tert*-butylbenzyl alcohol was reacted with 1 mol% $[1\text{-Cu}]BF_4$ and 7 mol% TEMPO the overall yield was 6% with a selectivity of 59 : 41 for the smaller substrate (Table 2, entry 1), whereas **6.3(NMI)** preferably oxidises the larger 3,5-di-*tert*-butyl-benzyl alcohol with a selectivity of 42 : 58 (entry 2). **10-(bipy)-2(NMI)** shows with 52 : 48 no preference (entry 3). Changing the smaller substrate to benzyl alcohol resulted in a comparable yield and a selectivity of 67 : 33 (entry 4). Again, the other two tested systems showed with 55 : 45 and 52 : 48 a smaller preference for the smaller substrate. Additional competition experiments of substrate pairs where the steric demand is further remote of the functional group and electronic differences are likely to be the cause of selectivity can be found in the ESI.† Although the effect is not too pronounced, these preliminary results show that there is a trend that $[1\text{-Cu}]BF_4$ preferably catalyses the conversion of the smaller substrate.

In conclusion, we have synthesised an organic cage whose *endo*-functionalised cavity offers three imidazole units. These can coordinate to copper(I), assembling a motif as it is observed in the active sites of many oxygenases. This complex is the first example of an imidazole employing mimic of non-heme enzymatic active sites offering histidine coordination that is assembled in the cavity of a molecular cage. We used a protocol based on catalytic

amounts of TEMPO for the catalytic oxidation of alcohols to aldehydes under aerobic conditions. The terminal oxidant in that protocol is oxygen. Preliminary results suggest that **[1-Cu]BF₄** preferably oxidises the smaller substrates in competition experiments. We believe that this trend can be improved significantly as **1** is easily accessible and therefore also easily altered.²⁰ Derivatisation of **1** has great potential to give mimics of ligand spheres of other enzymatic active sites involving histidine coordination. Our aim with this highly tunable system is to design detailed structural mimics that beside having interesting reactivities for itselfs may lead to a better understanding of these enzymes and consequently facilitate the specific design of new synthetic catalysts with unprecedented reactivities.

M. O. thanks the Deutsche Forschungsgemeinschaft (DFG, German Research Foundation) – OT 540/2-1 and the Fonds der Chemischen Industrie for funding. Prof. Dr Sven Schneider is highly acknowledged for his very generous support. We thank Prof. Dr Siegfried Schindler for the donation of Cu(MeCN)₄SbF₆.

Conflicts of interest

There are no conflicts to declare.

Notes and references

- 1 L. Ciano, G. J. Davies, W. B. Tolman and P. H. Walton, *Nat. Catal.*, 2018, **1**, 571.
- 2 V. C.-C. Wang, S. Maji, P. P.-Y. Chen, H. K. Lee, S. S.-F. Yu and S. I. Chan, *Chem. Rev.*, 2017, **117**, 8574.
- 3 E. I. Solomon, D. E. Heppner, E. M. Johnston, J. W. Ginsbach, J. Cirera, M. Qayyum, M. T. Kieber-Emmons, C. H. Kjaergaard, R. G. Hadt and L. Tian, *Chem. Rev.*, 2014, **114**, 3659.
- 4 S. I. Chan, Y.-J. Lu, P. Nagababu, S. Maji, M.-C. Hung, M. M. Lee, I.-J. Hsu, P. D. Minh, J. C.-H. Lai, K. Y. Ng, S. Ramalingam, S. S.-F. Yu and M. K. Chan, *Angew. Chem., Int. Ed.*, 2013, **52**, 3731.
- 5 (a) A. Kunishita, M. Kubo, H. Sugimoto, T. Ogura, K. Sato, T. Takui and S. Itoh, *J. Am. Chem. Soc.*, 2009, **131**, 2788; (b) C. Würtele, E. Gaoutchenova, K. Harms, M. C. Holthausen, J. Sundermeyer and S. Schindler, *Angew. Chem., Int. Ed.*, 2006, **45**, 3867; (c) M. Kumar, N. A. Dixon, A. C. Merkle, M. Zeller, N. Lehnert and E. T. Papish, *Inorg. Chem.*, 2012, **51**, 7004.
- 6 (a) C. F. Martens, R. J. M. Klein Gebbink, M. C. Feiters and R. J. M. Nolte, *J. Am. Chem. Soc.*, 1994, **116**, 5667; (b) J. A. Halfen, S. Mahapatra, E. C. Wilkinson, S. Kaderli, V. G. Young Jr, L. Que Jr, A. D. Zuberbühler and W. B. Tolman, *Science*, 1996, **271**, 1397; (c) C. Würtele, O. Sander, V. Lutz, T. Waitz, F. Tuczek and S. Schindler, *J. Am. Chem. Soc.*, 2009, **131**, 7544; (d) I. Garcia-Bosch, A. Company, J. R. Frisch, M. Torrent-Sucarrat, M. Cardellach, I. Gamba, M. Güell, L. Casella, L. Que Jr., X. Ribas, J. M. Luis and M. Costas, *Angew. Chem., Int. Ed.*, 2010, **49**, 2406; (e) C. Citek, C. T. Lyons, E. C. Wasinger and T. D. P. Stack, *Nat. Chem.*, 2012, **4**, 317; (f) R. Cao, C. Saracini, J. W. Ginsbach, M. T. Kieber-Emmons, M. A. Siegler, E. I. Solomon, S. Fukuzumi and K. D. Karlin, *J. Am. Chem. Soc.*, 2016, **138**, 7055; (g) V. E. Goswami, A. Walli, M. Förster, S. Dechert, S. Demeshko, M. C. Holthausen and F. Meyer, *Chem. Sci.*, 2017, **8**, 3031.
- 7 (a) M. Rolff, J. Schottenheim, G. Peters and F. Tuczek, *Angew. Chem., Int. Ed.*, 2010, **49**, 6438; (b) A. Hoffmann, C. Citek, S. Binder, A. Goos, M. Rüthausen, O. Troeppner, I. Ivanović-Burmazović, E. C. Wasinger, T. D. P. Stack and S. Herres-Pawlis, *Angew. Chem., Int. Ed.*, 2013, **52**, 5398; (c) K. V. N. Esguerra, Y. Fall, L. Petitjean and J.-P. Lumb, *J. Am. Chem. Soc.*, 2014, **136**, 7662; (d) A. Arnold, R. Metzinger and C. Limberg, *Chem. – Eur. J.*, 2015, **21**, 1198.
- 8 (a) S. Blanchard, L. Le Clainche, M.-N. Rager, B. Chansou, J.-P. Tuchagues, A. F. Duprat, Y. Le Mest and O. Reinaud, *Angew. Chem., Int. Ed.*, 1998, **37**, 2732; (b) G. N. Di Francesco, A. Gaillard, I. Ghiviriga, K. A. Abboud and L. J. Murray, *Inorg. Chem.*, 2014, **53**, 4647.
- 9 J.-N. Rebillé, B. Colasson, O. Bistri, D. Over and O. Reinaud, *Chem. Soc. Rev.*, 2015, **44**, 467.
- 10 (a) D. H. Leung, R. G. Bergman and K. N. Raymond, *J. Am. Chem. Soc.*, 2007, **129**, 2746; (b) P. Mal, B. Breiner, K. Rissanen and J. R. Nitschke, *Science*, 2009, **324**, 1697; (c) M. Yoshizawa, M. Tamura and M. Fujita, *Science*, 2006, **312**, 251; (d) S. Freye, J. Hey, A. Torras-Galán, D. Stalke, R. Herbst-Irmer, M. John and G. H. Clever, *Angew. Chem., Int. Ed.*, 2012, **51**, 2191; (e) Q. Zhang and K. Tieffenbacher, *J. Am. Chem. Soc.*, 2013, **135**, 16213; (f) M. Otte, *ACS Catal.*, 2016, **6**, 6491.
- 11 (a) I. Tabushi and Y. Kuroda, *J. Am. Chem. Soc.*, 1984, **106**, 4580; (b) A. Parrot, S. Collin, G. Bruylants and O. Reinaud, *Chem. Sci.*, 2018, **9**, 5479.
- 12 J. Baek, B. Rungtaeweevoranit, X. Pei, M. Park, S. C. Fakra, Y.-S. Liu, R. Matheu, S. A. Alshimir, S. Alshehri, C. A. Trickett, G. A. Somorjai and O. M. Yaghi, *J. Am. Chem. Soc.*, 2018, **140**, 18208.
- 13 (a) S. J. Lee, S.-H. Cho, K. L. Mulfort, D. M. Tiede, J. T. Hupp and S. T. Nguyen, *J. Am. Chem. Soc.*, 2008, **130**, 16828; (b) M. Otte, P. F. Kuijpers, O. Troeppner, I. Ivanović-Burmazović, J. N. H. Reek and B. de Bruin, *Chem. – Eur. J.*, 2013, **19**, 10170.
- 14 (a) J. Yang, B. Chatelet, V. Dufaud, D. Héroult, S. Michaud-Chevallier, V. Robert, J.-P. Dutasta and A. Martinez, *Angew. Chem., Int. Ed.*, 2018, **57**, 14212; (b) J. Yang, B. Chatelet, D. Héroult, J.-P. Dutasta and A. Martinez, *Eur. J. Org. Chem.*, 2018, 5618.
- 15 C. Coloban, V. Martin-Diaconescu, T. Parella, S. Goeb, C. García-Simón, J. Lloret-Fillol, M. Costas and X. Ribas, *Inorg. Chem.*, 2018, **57**, 3529.
- 16 (a) O. Francesconi, A. Ienco, G. Moneti, C. Nativi and S. Roelens, *Angew. Chem., Int. Ed.*, 2006, **45**, 6693; (b) B. Icli, N. Christinat, J. Tönnemann, C. Schüttler, R. Scopelliti and K. Severin, *J. Am. Chem. Soc.*, 2009, **131**, 3154.
- 17 L. Cao, O. Calderaru, A. C. Rosenzweig and U. Ryde, *Angew. Chem., Int. Ed.*, 2018, **57**, 162.
- 18 J. M. Hoover and S. S. Stahl, *J. Am. Chem. Soc.*, 2011, **133**, 16901.
- 19 Z. Liu, Z. Shen, N. Zhang, W. Zhong and X. Liu, *Catal. Lett.*, 2018, **148**, 2709.
- 20 M. Otte, M. Lutz and R. J. M. Klein Gebbink, *Eur. J. Org. Chem.*, 2017, 1657.

